

# Membrane electrode assemblies with low noble metal loadings for hydrogen production from solid polymer electrolyte water electrolysis

Huaneng Su, Vladimir Linkov and Bernard Jan Bladergroen

## Abstract

High performance membrane electrode assemblies (MEAs) with low noble metal loadings (NMLs) were developed for solid polymer electrolyte (SPE) water electrolysis. The electro- chemical and physical characterization of the MEAs was performed by  $IeV$  curves, electrochemical impedance spectroscopy (EIS) and scanning electron microscopy (SEM). Even though the total NML was lowered to  $0.38 \text{ mg cm}^{-2}$ , it still reached a high performance of  $1.633 \text{ V}$  at  $2 \text{ A cm}^{-2}$  and  $80^\circ \text{ C}$ , with  $\text{IrO}_2$  as anode catalyst. The influences of the ionomer content in the anode catalyst layer (CL) and the cell temperature were investigated with the purpose of optimizing the performance. SEM and EIS measurements revealed that the MEA with low NML has very thin porous cathode and anode CLs that get intimate contact with the electrolyte membrane, which makes a reduced mass transport limitation and lower ohmic resistance of the MEA. A short-term water electrolysis operation at  $1 \text{ A cm}^{-2}$  showed that the MEA has good stability: the cell voltage maintained at  $\sim 1.60 \text{ V}$  without distinct degradation after 122 h operation at  $80^\circ \text{ C}$  and atmospheric pressure.

## 1. Introduction

Solid polymer electrolyte water electrolysis (SPEWE) is a pleasing way for pure or 'green' hydrogen production at low temperature without fossil fuel consumption and emission of greenhouse gases such as  $\text{CO}_x$ ,  $\text{SO}_x$  and  $\text{NO}_x$  and any toxic particulates. Therefore, SPEWE is currently believed as a favorable technique for extensive hydrogen production in the future [1e3]. In recent years, although the researchers have speeded up the development of SPEWE, the systems are still too costly to replace traditional waterealkaline electrolyzers [1,3].

In conventional SPEWE technology, Ir (or  $\text{IrO}_2$ ) and Pt are commonly used noble metal catalysts respectively for the anode oxygen evolution reaction (OER) and the cathode hydrogen evolution reaction (HER) [3e10]. According to Millet et al. [3], these noble metal loadings (NMLs) require a significant reduction from a few mg

cm<sup>-2</sup> (current state-of-the-art) down to ca. 0.1 mg cm<sup>-2</sup> for the whole cost reduction. Therefore, many of the recent studies have been focusing on developing highly active anode and cathode catalysts for SPEWE [10e20] with reduced noble metals content and overall cost. For example, oxides such as IrRu [13,14], IrSn [15e17], IrTa [14,18], IrRuSn [19] and IrRuTa [20], etc. were developed as oxygen evolution electrocatalysts. Some of these catalysts showed much better performance for water electrolysis than the commonly used IrO<sub>2</sub> catalyst. However, it is still difficult to decrease the content of these noble metals to an acceptable level due to the unavailability of carbon support suitable for these catalysts [3,21]. On the other hand, some studies have intended to develop low-cost SPEs in place of the expensive Nafion<sup>®</sup> membrane [22e27]. Although significant performance values have been obtained in some studies, the practical use of these composite membranes under industrial electrolysis conditions has not been sufficiently demonstrated. For example, for non-homogeneous membrane, such as a Nafion<sup>®</sup> and PTFE reinforcement membrane, delamination of the MEA in 'harsh' environments such as hot water in a working electrolyzer should be considered since the thermal expansion and swelling coefficients of two polymers are different.

Like in low temperature hydrogen fuel cells, the MEA is the key part of an SPEWE system. The fabrication methods for MEAs with low NML (usually, Pt) have been studied extensively in the fuel cell technology to reduce the noble metal use and, accordingly, cost [28e30]. However, there has been limited work reported on developing MEAs with low NMLs for SPE water electrolysis, even though these two fields are closely related. One of the main reasons is the difficulty in fabricating thin (a few microns thick) and uniform anode catalyst layer (CL) due to the unavailability of supports suitable for the anode catalysts [3,21].

In our previous work, a novel catalyst coated membrane (CCM) method, termed catalyst sprayed membrane under illumination (CSMUI) [31], was developed for MEA preparation for SPEWE. The MEAs prepared by this method exhibited high performances for water electrolysis. In this study, we investigated the feasibility of using CSMUI method to prepare low NML MEAs for SPEWE. A high performance MEA with low NML was obtained using CSMUI method via further optimization of the anode CL structure. The effects of the NML and cell temperature on the cell performance were investigated. Polarization and durability tests showed that the MEA with low NML exhibited good performance and stability for SPE water electrolysis.

## **2. Experimental methods**

### **2.1 Preparation of MEAs**

The catalyst inks were prepared by mixing the catalysts powder into a blend of 5 wt.% Nafion<sup>®</sup> ionomer solution (DuPont, USA) and isopropanol. The catalyst used for the cathode and the anode were Hispec 4100 Pt/C (20 wt.% Pt, Alfa Aesar,

Johnson Matthey) and IrO<sub>2</sub> (99.9%, Alfa Aesar, Johnson Matthey), respectively. Before being used, the dispersion mixture was sonicated in a 40 kHz ultrasonic bath for 40 min. The polymer electrolyte membrane used in this study is Nafion<sup>®</sup> 212 (DuPont, USA). The membranes were pre-treated at 80 °C in the solutions of 5 wt.% H<sub>2</sub>O<sub>2</sub>, ultrapure water, 0.5 M H<sub>2</sub>SO<sub>4</sub> and ultrapure water for 60 min, sequentially.

The CCMs were obtained by spraying the catalyst inks onto the both side of the pretreated membranes with a spray gun (nozzle caliber: 0.2 mm, atomization style). A more detailed account of the preparation of the CCM has been given previously [31]. The Nafion<sup>®</sup> content varied from 0 wt.% to 30 wt.% in the anodes to be optimized, while it was always 30 wt.% in the cathodes for this study. The NMLs at the cathode and anode were determined by two ways. Firstly, the catalyst quantities for the cathode and anode inks were weighed accurately. Normally, 10% more catalyst than the calculated amount was used considering the loss during the fabrication process. Secondly, the uncoated membrane, the membrane coated with cathode CL, and the membrane coated with both cathode and anode CLs were weighted, whereby the individual NMLs for both the cathode and the anode can be calculated separately, to make sure that the NMLs conformed to the intended MEA design. Unless otherwise specified, the IrO<sub>2</sub> loading and Pt loading for the cathode and the anode were 0.04 and 0.4 mg cm<sup>-2</sup> respectively, much lower than for conventional SPEWE CCMs, amongst the lowest loadings for SPEWE that the authors have found in the literature [3,20,32].

Porous titanium (Ti) fiber (Bekenit, SaitamaKen, Japan; thickness 0.3 mm, 60% porosity) was used as the anode gas diffusion layer (GDL)/current collector. The GDL for the cathode was prepared with same procedure described in our previously work [31]. The active area of the prepared MEAs was 4 cm<sup>2</sup>.

## **2.2 Evaluation of MEA performance in water electrolysis**

An SPE water electrolysis cell was used to evaluate the performance of the as-prepared MEAs, and details of the cell can be found elsewhere [31]. The water electrolysis performance of the SPE electrolyzer was tested at 80 °C and atmospheric pressure. Preheated deionized water (18.3 MUcm), with a flow rate of 50 ml min<sup>-1</sup>, was circulated and supplied to the anode compartment by a peristaltic pump. The water temperature was kept at 5 °C higher than the cell temperature. Total cell polarization curves were recorded galvanostatically between 1 mA cm<sup>-2</sup> and 2 A cm<sup>-2</sup> using a Neware battery testing system (Neware Technology Ltd, China).

### **2.3 SEM and electrochemical measurements of MEAs**

An ultra-high resolution field-emission SEM (Nova™ NanoSEM 230, FEI, USA) was used to observe the cross-sections and surfaces of the MEAs.

Electrochemical impedance spectroscopy (EIS) was performed by an Autolab PGSTAT 30 Potentiostat/Galvanostat (Metrohm) equipped with a 10 A booster and a frequency response analyzer (FRA). The impedance data were generated and simulated using the Autolab Nova software. During EIS tests, the cathode was served as both the reference electrode (RE) and the counter electrode (CE) since the polarization of HER is negligible compared to that for OER at anode during water electrolysis operation. The impedance spectra were recorded at a cell potential of 1.5 V in the frequency range of 0.1e10,000 Hz with sinusoidal amplitude of 5 mV.

## **3. Results and discussion**

### **3.1 Water electrolysis performance of the MEAs with different NMLs**

Through gradually decreasing the IrO<sub>2</sub> loading on the anode and Pt loading on the cathode, a series of MEAs with different NMLs were prepared. Table 1 shows the specifications of these MEAs. For simplicity, they were designated in shortened form as MEA-1, MEA-2, MEA-3 and MEA-4, respectively.

Fig. 1 shows the performance of the MEAs with various amounts of NML. It is obvious that the cell voltage rose considerably in the activation overpotential region with the decrease of catalyst loading, indicating that a slow electrode kinetics leads to performance loss. At a current of 0.3 A cm<sup>-2</sup>, the cell voltage of MEA-3 reached 1.474 V, 35 mV higher than that of MEA-1 (1.439 V). However, with the increase in current density, the cell voltage difference between MEA-3 and MEA-1 became gradually less significant. At a current of 2 A cm<sup>-2</sup>, the cell voltage of MEA-3 was 1.633 V, only 3 mV higher than that of MEA-1 (1.63 V). By contrast, at high current densities, the cell voltage is generally affected by bubble formation (known as bubble overpotential) and ohmic resistivity, thus giving a determination of the MEA performance under practical operation conditions. Therefore, the significant improvement of water electrolysis performance in the medium and high current density region (>1 A cm<sup>-2</sup>) indicates that MEA-3 with an NML of 0.38 mg cm<sup>-2</sup> possesses lower ohmic resistance and mass transport limitations. This result indicates that high performance MEA with low NML for SPE water electrolysis can be obtained by minimizing the mass transport and electronic-resistance of the system.

It should be pointed out that a further decrease of NML from 0.38 mg cm<sup>-2</sup> to 0.28 mg cm<sup>-2</sup> (MEA-4) shows no MEA performance gains, either at low or high current densities, which could be due to two possible reasons: (1) catalyst insufficiency limits the electrochemical reactions in the electrodes at high current

densities; (2) too little catalysts lead to poor contact between the CLs and the membrane, as well as the CLs and the backing layers.

Fig. 2(A) shows the in situ impedance curves of the four MEAs at a cell voltage of 1.5 V. It can be seen that only one low-frequency response arc was detected, indicating that mass transport limitation was negligible in this operation [3]. Then a widely employed equivalent circuit (EC) [3,33] can be used to fit the impedance data according to the assignment of Nyquist plot features, as shown in Fig. 2(B). The low-frequency response arc is attributed to the anode charge transfer processes and represented by a resistor  $R_{CT,A}$ . The constant phase element (CPE) in parallel to  $R_{CT,A}$  represents the double-layer capacitance for the anode. The high-frequency response arc is attributed to cathode process and represented by a resistance ( $R_{CT,C}$ ) in parallel with a CPE. Although similar high-frequency feature can be found in some published works

Table 1 – Composition of MEAs.			
MEA	Anode <sup>a</sup> (IrO <sub>2</sub> )	Cathode <sup>b</sup> (20 wt.% Pt/C)	Noble metal loading (Ir + Pt)
MEA-1	2.0 mg cm <sup>-2</sup>	1.0 mg cm <sup>-2</sup>	1.91 mg cm <sup>-2</sup>
MEA-2	1.0 mg cm <sup>-2</sup>	0.5 mg cm <sup>-2</sup>	0.96 mg cm <sup>-2</sup>
MEA-3	0.4 mg cm <sup>-2</sup>	0.2 mg cm <sup>-2</sup>	0.38 mg cm <sup>-2</sup>
MEA-4	0.3 mg cm <sup>-2</sup>	0.15 mg cm <sup>-2</sup>	0.28 mg cm <sup>-2</sup>

a Nafion<sup>®</sup> content: 5 wt.%.  
b Nafion<sup>®</sup> content: 30 wt.%.

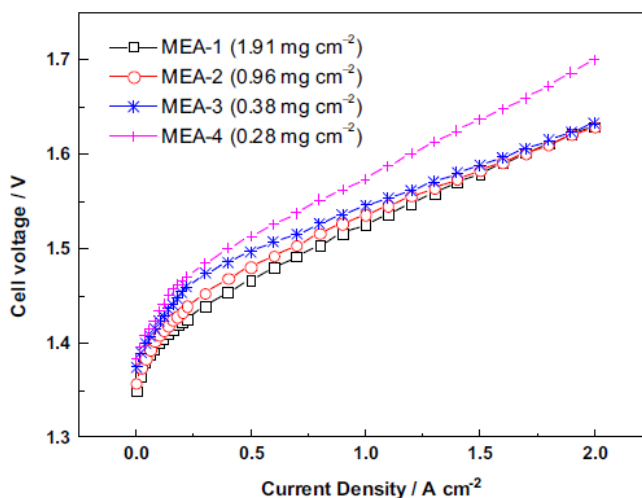


Fig. 1 – Water electrolysis performances of MEAs with various NMLs, evaluated at a cell temperature of 80 °C and atmospheric pressure. The weight/area values in the legend refer to the NML.

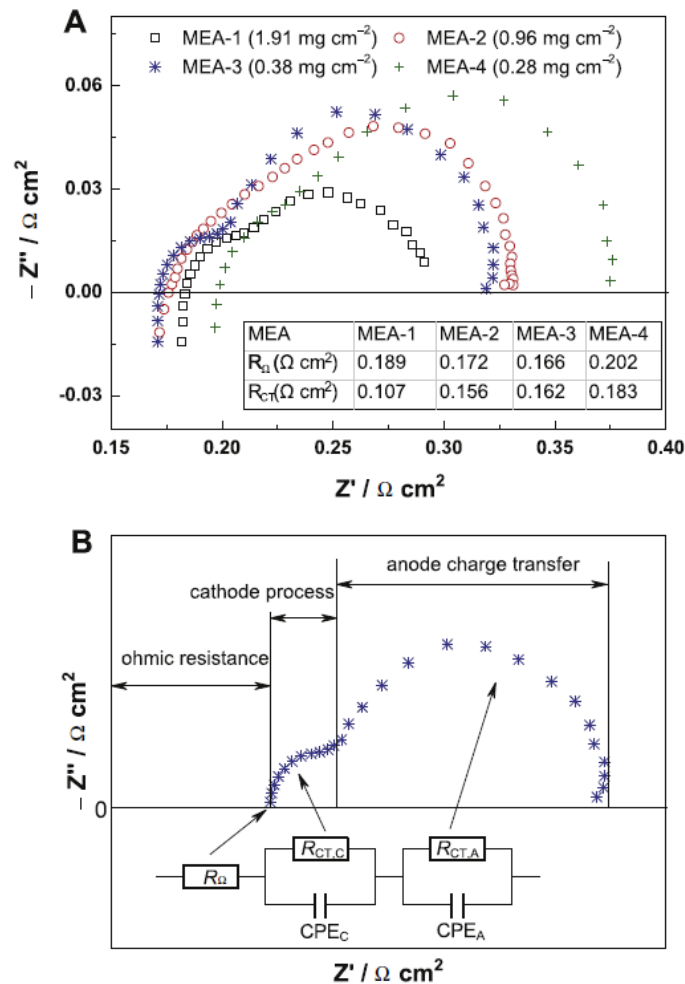


Fig. 2 – (A) In situ impedance curves of MEAs with various NMLs at 80 °C and 1.5 V. (B) Assignment of Nyquist plot features (MEA-3 as example) and the equivalent circuit for SPE water electrolysis. The weight/area values in the legend refer to the NML.

[6,8], the origin of the high-frequency impedance response has not been conclusively established [34], MEA structure features (such as the proton conductivity limitation within the CL) are suspected to be the reasons for this phenomenon [33,35]. The total charge transfer resistance ( $R_{CT}$ ) was then obtained by adding up  $R_{CT,C}$  and  $R_{CT,A}$ . The high-frequency intercept on the real axis,  $R_U$ , comprises ionic resistances of the membrane and the CLs, electronic resistances of each cell component (i.e. CLs, backing layers and bipolar plates) and the interfacial contact resistances between them.

Through simulation with the EC, the cell resistance ( $R_U$ ) and total charge transfer resistance ( $R_{CT}$ ) of the four MEAs can be calculated and are also summarized in an inset table in Fig. 2(A). It is clear that MEA-4 had the largest ohmic resistance and charge transfer resistance, which may due to the

insufficient catalyst loading of this MEA resulting in poor electrochemical reaction kinetics. However, MEA-3 with a relative low NML ( $0.38 \text{ mg cm}^{-2}$ ) showed the lowest ohmic resistance compared to MEA-1 and MEA-2, which may result from the reductions on both the ionic- and electronic-resistances of the anode CL since all other components and test conditions were identical in the study, indicating that decreasing the catalyst loading is an effective way to lower ohmic resistance of the CL due to decreased CL thickness. The  $R_U$  order of the four MEAs is certainly consistent with their performance shown in Fig. 1: the lower the cell resistance, the better the performance improvement at high current densities, which suggests that lowering cell resistance is a key factor to obtaining high performance MEAs for SPE water electrolysis, especially in practical applications (normally operated at medium and high current densities). These findings are in good agreement with those reported by Rasten et al. [8].

The utilization efficiency of the noble metal is shown in Fig. 3, in which the polarization curves from Fig. 1 are plotted against the mass activity (A/mg of noble metal) as  $x$ -axis. The MEAs with lower NMLs (MEA-3 and MEA-4) show significantly higher utilization efficiency than the MEAs with normal NMLs (MEA-1 and MEA-2), which implies that the CSMUI method is effective in preparation of low NMLs MEAs for SPE water electrolysis. The MEA with a  $0.38 \text{ mg cm}^{-2}$  (MEA-3) shows the highest utilization efficiency, in which the NML is only  $1/5 \times 10^{-1}$  of that in normal MEAs ( $2 \times 10^{-3} \text{ mg cm}^{-2}$ ), indicating that high performance SPE water electrolyzer MEAs with low NML can be obtained by optimizing the fabrication and structure of the catalyst layer.

### **3.2. Optimization of Nafion<sup>®</sup> content in the anode CL of the MEAs with low NML**

Nafion<sup>®</sup> ionomer is a key component in the CLs, and functional to form the desired three-phase reaction boundaries and boost catalysts utilization in the electrodes. For Pt/C catalyst,  $\sim 30 \text{ wt.}\%$  Nafion<sup>®</sup> content is an optimal value in CL, which has been widely used in PEMFC studies [36]. However, the optimal value for IrO<sub>2</sub> catalyst, which has been extensively used in SPE water electrolyzers [4e9], has not been reported yet. In current literature on SPE water electrolysis, there is no recognized value for the Nafion<sup>®</sup> content in the anode, typically 5-33 wt.% Nafion<sup>®</sup> content was applied [8,9,13e16,18,20,37].

Fig. 4 presents polarization curves of the MEAs with various Nafion<sup>®</sup> content in the anode CL. The Nafion<sup>®</sup> content at the cathode for all these MEAs was 30 wt.%. For comparison purposes, the cell voltages of the MEAs at  $1 \text{ A cm}^{-2}$  with various Nafion<sup>®</sup> contents were plotted, as shown in the insert of Fig. 4. It is evident that the Nafion<sup>®</sup> content in the anode CL has an obvious influence on the performance of

the MEA with low NML. With the decrease of the Nafion<sup>®</sup> content from 30 wt.% to 5 wt.%, the performance of the MEA increased by about 70%, and the current density at 1.6 V increased from 0.98 A cm<sup>-2</sup> to 1.63 A cm<sup>-2</sup>. Generally, the electronic conductivity and the porosity of CL improve with a decrease in Nafion<sup>®</sup> ionomer content, which certainly helps the improvement of the MEA performance. However, too low content of Nafion<sup>®</sup> greatly decreases the three-phase reaction boundaries in the CL, which in turn affects the MEA performance adversely.

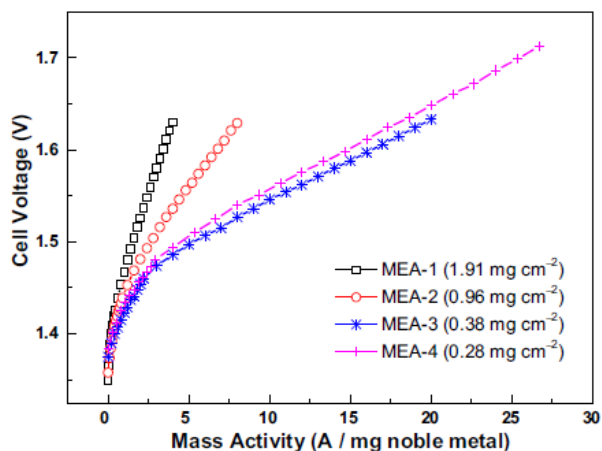


Fig. 3 – Comparison of the specific activities (per mg of noble metal) of the MEAs with various NMLs. The membrane designations in the legend and the test conditions are same as in Fig. 1.

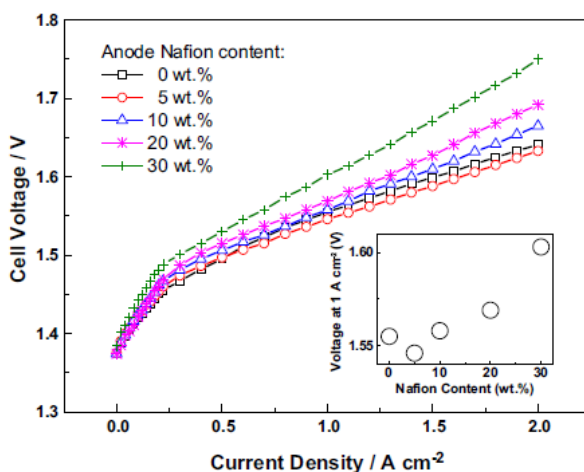


Fig. 4 – The effect of Nafion<sup>®</sup> content in anode CL on the water electrolysis performance of the MEA with low NML (0.38 mg cm<sup>-2</sup>). The Nafion<sup>®</sup> content in cathode CL was fixed at 30 wt.%. All data were collected at a cell temperature of 80 °C and at atmospheric pressure.



Under conditions used in the study, it was found that the MEA with the lowest Nafion<sup>®</sup> content (5 wt.%) exhibited the highest performance due to possible reasons as follows.

- i. Unlike Pt/C catalyst, the nano IrO<sub>2</sub> catalyst is denser due to the absence of electrocatalyst support material, theoretically the required ionomer should be lower.
- ii. The CSMUI method results in ample interfacial contact between the CL and the membrane and IrO<sub>2</sub> catalyst mainly located in the catalyst/membrane interface, thus the optimal Nafion<sup>®</sup> content in CL can be decreased greatly. This can be verified by comparing the performance of the MEA without Nafion<sup>®</sup> ionomer in the CL. From Fig. 4, it can be seen that the MEA with 0 wt.% Nafion<sup>®</sup> content in the anode still delivered a high performance, only next to the MEA with 5 wt.% Nafion<sup>®</sup> content, which indicates that the Nafion<sup>®</sup> ionomer from the electrolyte surface is almost enough for proton transfer in anode CL.
- iii. The MEA with low NML possesses a very thin CL, so the loss of the three-phase reaction boundaries due to the low Nafion<sup>®</sup> content might be negligible since the electrochemical reaction occurs mainly in the catalyst/membrane interface [30,38].
- iv. In SPE water electrolysis, the most important limitation of the MEA cell is its high electrical resistance, as has been proven by Rasten et al. [8]. There was a concern that too low content of Nafion<sup>®</sup> in CL may decrease the adhesive force between the CL and the membrane, leading to delamination of the CL from the surface of membrane [39]. Considering this, a stability test was performed (see Section 3.4) and it was found that the low NML MEA still had good CL/membrane interface and performance stability even after the 120 h test, which further indicates that the CSMUI method can produce strong catalyst/membrane bond, thus forming a tight catalyst/ membrane interface even though the content of Nafion<sup>®</sup> binder in the catalyst ink is low.

Based on above reasons, it is concluded that the optimum anode Nafion<sup>®</sup> content for the low NML MEA with IrO<sub>2</sub> catalyst is 5 wt.%. This value was also used by several authors where MEAs showed high performance values [15,16,20].

### **3.3. Effect of cell temperature on the performance of the MEA with low NML**

It is widely recognized that major polarization occurs in the anode of SPE electrolyzer due to poor OER kinetics and limitations in proton transfer within the CL of the MEA. Therefore, elevated operating temperatures are required to obtain better cell performance. Considering the normal working temperature region for the Nafion<sup>®</sup>-based water electrolysis system, the cell temperatures varied from 25 °C to 90 °C were evaluated. Taking into account the NML considerations presented

above, the MEA was prepared with  $0.38 \text{ mg cm}^{-2}$  NML and 5 wt.% Nafion<sup>®</sup> content in the anode CL.

Fig. 5(A) shows the performance of the MEA with low NML at various temperatures. It clearly demonstrates that the MEA performance improved by increasing the cell temperature, resulting from the improved diffusion processes and the electrode kinetics, as well as an increase in electrolyte conductivity [24,40]. Also, it found that the temperature effect on the enhancement of the cell performance was lower in the region above  $60 \text{ }^{\circ}\text{C}$ . As shown in Fig. 5(B), when the cell temperature increased from  $25 \text{ }^{\circ}\text{C}$  to  $60 \text{ }^{\circ}\text{C}$ , the cell voltage decreased by 154 mV (from 1.724 V to 1.57 V). Further increasing the temperature to  $90 \text{ }^{\circ}\text{C}$  only causes a cell voltage decrease of 32 mV from 1.57 V to 1.538 V.

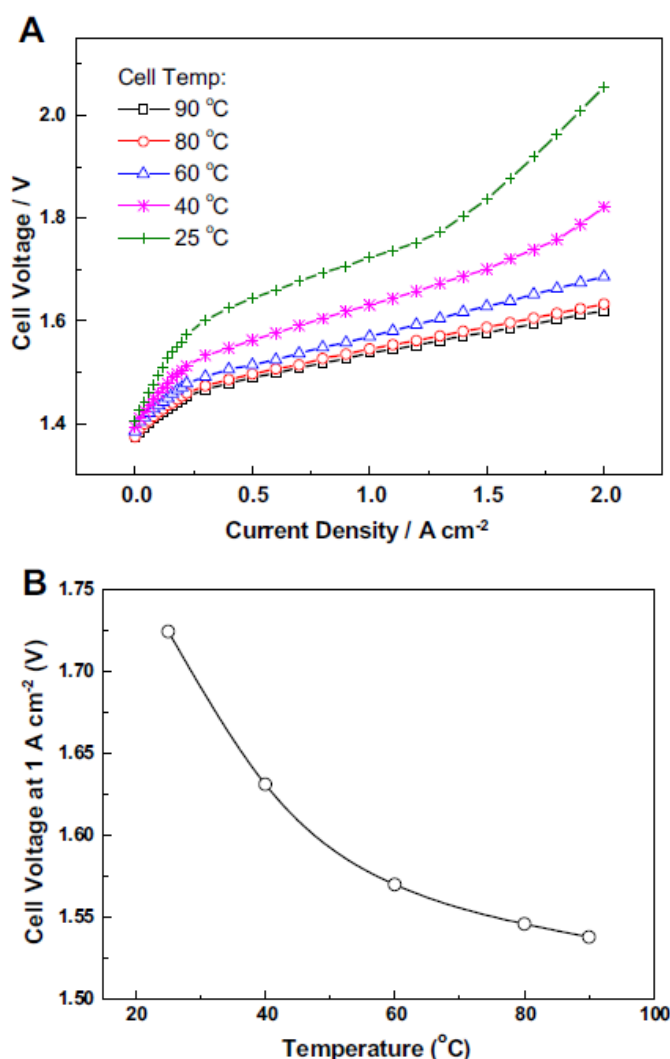


Fig. 5 – Effect of cell temperature on the water electrolysis performance of the MEA with low NML ( $0.38 \text{ mg cm}^{-2}$ ): (A) polarization curves at various cell temperatures; (B) cell voltage at  $1 \text{ A cm}^{-2}$  versus cell temperature.

**Table 2 – Influence of the cell temperature on the kinetic parameters of the low NML MEA.**

Parameter	Temperature/°C				
	25	40	60	80	90
$a$ (mV)	1468.61	1438.77	1402.17	1382.47	1371.24
$b$ (mV dec <sup>-1</sup> )	39.27	38.05	37.24	36.85	36.81
$R$ ( $\Omega$ cm <sup>2</sup> )	0.215	0.152	0.116	0.108	0.105
$\times 10^7 j_0$ (mA cm <sup>-2</sup> )	8.23	21.40	35.81	41.62	45.10

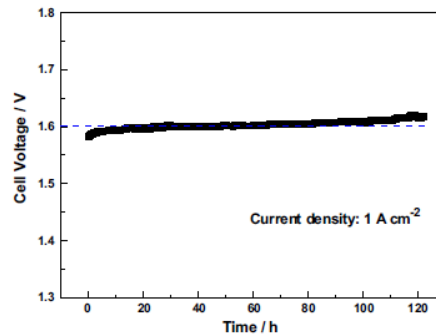


Fig. 6 – 122 h water electrolysis test of the MEA with low NML operated at 80 °C, 1 atm and 1 A cm<sup>-2</sup>.

In order to elucidate these results, a semiempirical equation [39,41e43] was used to fit these experimental data, which is written as:

$$E = a + b \cdot \log(j) + R \cdot j; \quad (1)$$

where  $E$  is the experimental cell potential,  $a$  is a constant,  $b$  is the Tafel slope which is related to the performance of the CL while the electro-catalytic reaction is the rate determining step,  $R$  is the uncompensated ohmic resistance, and  $j$  is the current density. At low current density, where  $R$  can be neglected,  $a$  and  $b$  can be found from the slope of the curve. By using the following expression [42]:

$$E_r = a + b \cdot \log j_0; \quad (2)$$

the exchange current density ( $j_0$ ) can be obtained from  $a$ , which is a measure of electrocatalytic activity, related to the OER reaction rate [42]. In Eq. (2),  $E_r$  is the thermodynamic reversible potential. The values of these parameters are shown in Table 2.

As expected, a rise of cell temperature obviously increased the exchange current density ( $j_0$ ) due to the intrinsic enhancement of the catalytic activity with temperature. It was found that the cell ohmic resistance,  $R$ , decreased with an increase in temperature. Generally, the influence of temperature on the electronic conductivity of the CLs is limited, thus the change of  $R$  values mostly depends upon the proton conductivity in the CLs and the membrane. However, since the conductivity of Nafion<sup>®</sup> ionomer depends crucially on the water content, an elevation in temperature at its “high” region has less influence on the proton conductivity in water-rich surroundings due to improved “water activity” [44,45], which could be the reason that  $R$ -changes slightly at higher temperatures. Furthermore, Nafion<sup>®</sup> ionomer is also an active component in the electrodes, by which protons can be transported in the CLs. Consequently, the slight increase in the Tafel slope ( $b$ ) can also be observed when the temperature reaches 60 °C.

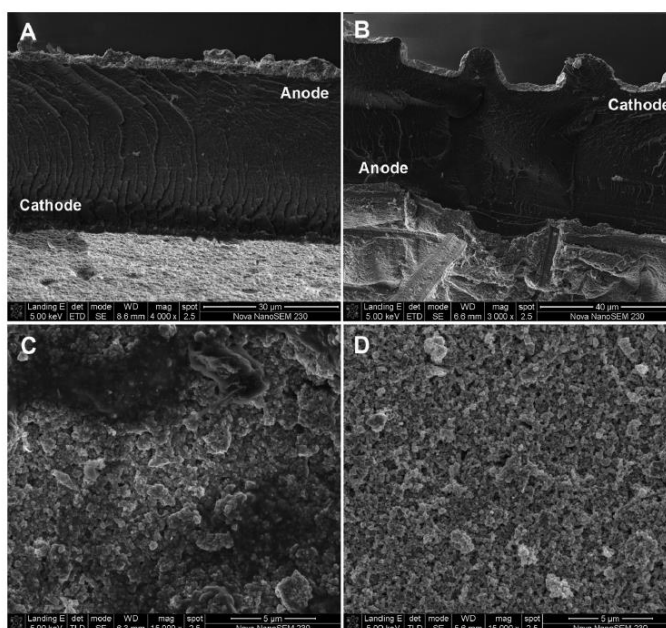


Fig. 7 – SEM micrographs showing the cross-sections of the fresh MEA (A) and the MEA after durability test (B), the surface morphologies of the anode CL (C) and the cathode CL (D) of the MEA after durability test.

At low cell temperatures (<60 °C), the inefficiencies of the proton transfer and electrode kinetics are thought to be the main reasons for the performance deterioration, especially at high current densities. Taking these findings into account, the operating temperature for the low NML MEA should be above 60 °C, where the MEA can reach satisfactory performance due to considerable electrode kinetics and proton conductivity values.

### 3.4. Durability of the MEA with low NML

In order to investigate the durability of the MEA with low NML, a primary 122 h water electrolysis operation test at 1 A cm<sup>-2</sup> and 80 °C was conducted, as shown in Fig. 6.

The MEA used in this test had the same composition as the MEA-3 listed in Table 1, i.e., the total NML was  $0.38 \text{ mg cm}^{-2}$  and the anode Nafion<sup>®</sup> content was 5 wt.%. It can be observed that the cell voltage remains at  $\sim 1.60 \text{ V}$  without significant cell voltage decay during the 122 h operation at  $80 \text{ }^{\circ}\text{C}$  and a normal working current density of  $1 \text{ A cm}^{-2}$ , implying the good stability of the low NML MEA in this study. The ‘apparent’ degradation of the MEA performance estimated from Fig. 6 is ca.  $230 \text{ mV h}^{-1}$ , which is similar to value in our previous study for the MEA with normal NML [31]. It can be assumed that the stability of the MEA profited from the uniform porous structure of the CLs, as well as the good contact between the CLs and the Nafion<sup>®</sup> membrane caused by the CSMUI deposition method. To verify this result, the cross-section of the MEA which endured 122 h durability test was compared with that of an as-prepared MEA using SEM, as shown in Fig. 7. Fig. 7(A) shows the cross section of an untested MEA, in which it can be seen that the CLs closely adhered to the electrolyte membrane. Even after 122 h water electrolysis, no CL piece peeled from the membrane (Fig. 7(B)), indicating that the CLs remained stucked to the electrolyte membrane strongly during electrolysis, which confirmed the validity of CSMUI method used for the low NML MEAs fabrication. Furthermore, from Fig. 7(A) the thickness of cathode and anode CLs of about 3.5 mm and 1.6 mm, respectively were estimate. Such thin CLs may lead to small mass transport and charge transfer resistances, which further confirmed the results presented in Figs. 1 and 2. Fig. 7(C) and (D) showed the uniform porous structures of the CLs, which are certainly beneficial to water transport and departure of gases. The combination of thin CLs, uniformly porous CL structure and close contact between the membrane and the CLs could be the reasons why the MEA with low NML exhibited good performance and stability in SPE water electrolysis.

#### 4. Conclusions

High performance MEA with low NML was prepared for SPE water electrolysis using the CSMUI method. The optimal Nafion<sup>®</sup> content in the anode was only 5 wt.%, with a total NML of  $0.38 \text{ mg cm}^{-2}$ . These values are significantly lower than those for the MEAs usually reported, suggesting ample interface contact between the membrane and the CLs. Compared with conventional MEAs, the MEA with low NML showed much higher mass activity, especially at high current densities, due to a decrease in ohmic resistance and mass transport limitations. It was also found that the working operating temperature for the low NML MEA should be above  $60 \text{ }^{\circ}\text{C}$ , where the MEA can reach a satisfactory performance due to improved electrode kinetics and proton conductivity. At the working temperature of  $80 \text{ }^{\circ}\text{C}$ , the cell voltage can be as low as  $1.546 \text{ V}$  at  $1 \text{ A cm}^{-2}$  whereby the terminal voltage was only  $1.633 \text{ V}$  at  $2 \text{ A cm}^{-2}$ , which are comparable to the results found for the MEAs with standard NMLs. The durability test showed that the MEA with low NML exhibited

good stability in water electrolysis and at a current of  $1 \text{ A cm}^{-2}$  its voltage remained at  $\sim 1.60 \text{ V}$  without significant degradation during the 122 h of testing. It is suggested that the thin CLs, the uniformly porous CL structure, as well as the ample interfacial contact between the membrane and the CLs may be crucial factors yielding high performance and good stability of the newly prepared MEAs.

### **Acknowledgments**

The authors acknowledge the financial support from the NRF Innovation Postdoctoral Fellowship (Grant No: 76466).

## References

- [1] Muradov NZ, Veziro\_glu TN. "Green" path path from fossil-based to hydrogen economy: an overview of carbon-neutral technologies. *Int J Hydrogen Energy* 2008;33(23):6804e39.
- [2] Grigoriev S, Poremsky V, Fateev V. Pure hydrogen production by PEM electrolysis for hydrogen energy. *Int J Hydrogen Energy* 2006;31(2):171e5.
- [3] Millet P, Mbemba N, Grigoriev SA, Fateev VN, Aukauloo A, Etie' vant C. Electrochemical performances of PEM water electrolysis cells and perspectives. *Int J Hydrogen Energy* 2011;36(6):4134e42.
- [4] Slavcheva E, Radev I, Bliznakov S, Topalov G, Andreev P, Budevski E. Sputtered iridium oxide films as electrocatalysts for water splitting via PEM electrolysis. *Electrochim Acta* 2007;52(12):3889e94.
- [5] Hu J-M, Zhang J-Q, Cao C-N. Oxygen evolution reaction on IrO<sub>2</sub>-based DSA<sup>®</sup> type electrodes: kinetics analysis of Tafel lines and EIS. *Int J Hydrogen Energy* 2004;29(8):791e7.
- [6] Siracusano S, Baglio V, Stassi A, Ornelas R, Antonucci V, Arico` AS. Investigation of IrO<sub>2</sub> electrocatalysts prepared by a sulfite-couplex route for the O<sub>2</sub> evolution reaction in solid polymer electrolyte water electrolyzers. *Int J Hydrogen Energy* 2011;36(13):7822e31.
- [7] Song S, Zhang H, Ma X, Shao Z, Baker RT, Yi B. Electrochemical investigation of electrocatalysts for the oxygen evolution reaction in PEM water electrolyzers. *Int J Hydrogen Energy* 2008;33(19):4955e61.
- [8] Rasten E, Hagen G, Tunold R. Electrocatalysis in water electrolysis with solid polymer electrolyte. *Electrochim Acta* 2003;48(25e26):3945e52.
- [9] Cruz J, Baglio V, Siracusano S, Ornelas R, Ortiz-Frade L, Arriaga L, et al. Nanosized IrO<sub>2</sub> electrocatalysts for oxygen evolution reaction in an SPE electrolyzer. *J Nanopart Res* 2011;13(4):1639e46.
- [10] Grigoriev SA, Millet P, Fateev VN. Evaluation of carbon-evolution reaction in PEM water electrolyzers. *J Power Sources* 2008;177(2):281e5.
- [11] Cheng JB, Zhang HM, Ma HP, Zhong HX, Zou Y. Study of carbon-supported IrO<sub>2</sub> and RuO<sub>2</sub> for use in the hydrogen evolution reaction in a solid polymer electrolyte electrolyzer. *Electrochim Acta* 2010;55(5):1855e61.
- [12] Grigoriev SA, Mamat MS, Dzhus KA, Walker GS, Millet P. Platinum and palladium nano-particles supported by graphitic nano-fibers as catalysts for PEM water electrolysis. *Int J Hydrogen Energy* 2011;36(6):4143e7.
- [13] Cheng J, Zhang H, Chen G, Zhang Y. Study of Ir<sub>x</sub>Ru<sub>1-x</sub>O<sub>2</sub> oxides as anodic electrocatalysts for solid polymer electrolyte water electrolysis. *Electrochim Acta* 2009;54(26):6250e6.
- [14] Di Blasi A, D'Urso C, Baglio V, Antonucci V, Arico AS, Ornelas R, et al. Preparation and evaluation of RuO<sub>2</sub>eIrO<sub>2</sub>, IrO<sub>2</sub>ePt and IrO<sub>2</sub>eTa<sub>2</sub>O<sub>5</sub> catalysts for the oxygen evolution reaction in an SPE electrolyzer. *J Appl Electrochem* 2009;39(2):191e6.

- [15] Marshall A, Børresen B, Hagen G, Tsyarkin M, Tunold R. Electrochemical characterisation of  $\text{Ir}_x\text{Sn}_{1-x}\text{O}_2$  powders as oxygen evolution electrocatalysts. *Electrochim Acta* 2006;51(15):3161e7.
- [16] Marshall A, Børresen B, Hagen G, Sunde S, Tsyarkin M, Tunold R. Iridium oxide-based nanocrystalline particles as oxygen evolution electrocatalysts. *Russ J Electrochem* 2006;42(10):1134e40.
- [17] Marshall A, Børresen B, Hagen G, Tsyarkin M, Tunold R. Preparation and characterisation of nanocrystalline  $\text{Ir}_x\text{Sn}_{1-x}\text{O}_2$  electrocatalytic powders. *Mater Chem Phys* 2005;94(2e3):226e32.
- [18] Siracusano S, Baglio V, D'Urso C, Antonucci V, Arico AS. Preparation and characterization of titanium suboxides as conductive supports of  $\text{IrO}_2$  electrocatalysts for application in SPE electrolyzers. *Electrochim Acta* 2009;54(26):6292e9.
- [19] Vazquez-Gomez L, Ferro S, De Battisti A. Preparation and characterization of  $\text{RuO}_2\text{eIrO}_2\text{eSnO}_2$  ternary mixtures for advanced electrochemical technology. *Appl Catal B* 2006;67(1e2):34e40.
- [20] Marshall AT, Sunde S, Tsyarkin M, Tunold R. Performance of a PEM water electrolysis cell using  $\text{Ir}_x\text{Ru}_y\text{Ta}_z\text{O}_2$  electrocatalysts for the oxygen evolution electrode. *Int J Hydrogen Energy* 2007;32(13):2320e4.
- [21] Millet P, Ngameni R, Grigoriev SA, Fateev VN. Scientific and engineering issues related to PEM technology: water electrolyzers, fuel cells and unitized regenerative systems. *Int J Hydrogen Energy* 2011;36(6):4156e63.
- [22] de Souza RF, Padilha JC, Gonç alves RS, de Souza MO, Rault-Berthelot J. Electrochemical hydrogen production from water electrolysis using ionic liquid as electrolytes: towards the best device. *J Power Sources* 2007;164(2):792e8.
- [23] Yang LJ, Su HN, Shu T, Liao SJ. Enhanced electro-oxidation of formic acid by a PdPt bimetallic catalyst on a  $\text{CeO}_2$ -modified carbon support. *Sci China Chem* 2012;55(3):391e7.
- [24] Antonucci V, Di Blasi A, Baglio V, Ornelas R, Matteucci F, Ledesma-Garcia J, et al. High temperature operation of a composite membrane-based solid polymer electrolyte water electrolyser. *Electrochim Acta* 2008;53(24):7350e6.
- [25] Baglio V, Ornelas R, Matteucci F, Martina F, Ciccarella G, Zama I, et al. Solid polymer electrolyte water electrolyser based on Nafion- $\text{TiO}_2$  composite membrane for high temperature operation. *Fuel Cells* 2009;9(3):247e52.
- [26] Wei GQ, Xu L, Huang CD, Wang YX. SPE water electrolysis with SPEEK/PES blend membrane. *Int J Hydrogen Energy* 2010;35(15):7778e83.
- [27] Sawada S, Yamaki T, Maeno T, Asano M, Suzuki A, Terai T, et al. Solid polymer electrolyte water electrolysis systems for hydrogen production based on our newly developed membranes, part I: analysis of voltage/current characteristics. *Prog Nucl Energy* 2008;50(2e6):443e8.
- [28] Su HN, Liao SJ, Shu T, Gao HL. Performance of an ultra-low platinum loading membrane electrode assembly prepared by a novel catalyst-sprayed membrane technique. *J Power Sources* 2010;195(3):756e61.



- [29] Wee JH, Lee KY, Kim SH. Fabrication methods for low-Pt-loading electrocatalysts in proton exchange membrane fuel cell systems. *J Power Sources* 2007;165(2):667e77.
- [30] Su H-N, Zeng Q, Liao S-J, Wu Y-N. High performance membrane electrode assembly with ultra-low platinum loading prepared by a novel multi catalyst layer technique. *Int J Hydrogen Energy* 2010;35(19):10430e6.
- [31] Su H, Bladergroen BJ, Linkov V, Pasupathi S, Ji S. Study of catalyst sprayed membrane under irradiation method to prepare high performance membrane electrode assemblies for solid polymer electrolyte water electrolysis. *Int J Hydrogen Energy* 2011;36(23):15081e8.
- [32] Su H, Bladergroen BJ, Pasupathi S, Linkov V, Ji S. Performance investigation of membrane electrode assemblies for hydrogen production by solid polymer electrolyte water electrolysis. *Int J Electrochem Sci* 2012;7(5):4223e34.
- [33] Yuan XZ, Wang HJ, Sun JC, Zhang JJ. AC impedance technique in PEM fuel cell diagnosis e a review. *Int J Hydrogen Energy* 2007;32(17):4365e80.
- [34] Malevich D, Halliop E, Peppley BA, Pharoah JG, Karan K. Investigation of charge-transfer and mass-transport resistances in PEMFCs with microporous layer using electrochemical impedance spectroscopy. *J Electrochem Soc* 2009;156(2):B216.
- [35] Freire TJP, Gonzalez ER. Effect of membrane characteristics and humidification conditions on the impedance response of polymer electrolyte fuel cells. *J Electroanal Chem* 2001;503(1e2):57e68.
- [36] Sasikumar G, Ihm JW, Ryu H. Dependence of optimum Nafion content in catalyst layer on platinum loading. *J Power Sources* 2004;132(1e2):11e7.
- [37] Wei G, Wang Y, Huang C, Gao Q, Wang Z, Xu L. The stability of MEA in SPE water electrolysis for hydrogen production. *Int J Hydrogen Energy* 2010;35(9):3951e7.
- [38] Su H-N, Liao S-J, Wu Y-N. Significant improvement in cathode performance for proton exchange membrane fuel cell by a novel double catalyst layer design. *J Power Sources* 2010;195(11):3477e80.
- [39] Ma L, Sui S, Zhai Y. Investigations on high performance proton exchange membrane water electrolyzer. *Int J Hydrogen Energy* 2009;34(2):678e84.
- [40] Xu W, Scott K, Basu S. Performance of a high temperature polymer electrolyte membrane water electrolyser. *J Power Sources* 2011;196(21):8918e24.
- [41] Kelly NA, Gibson TL, Cai M, Spearot JA, Ouwerkerk DB. Development of a renewable hydrogen economy: optimization of existing technologies. *Int J Hydrogen Energy* 2010;35(3):892e9.
- [42] Rasten E. Electrocatalysis in water electrolysis with solid polymer electrolyte. Norwegian University of Science and Technology; 2001.
- [43] Lobato J, Cañ izares P, Rodrigo MA, Linares JJ, Ú beda D, Pinar FJ. Study of the catalytic layer in polybenzimidazole-based high temperature PEMFC: effect of platinum content on the carbon support. *Fuel Cells* 2010;10(2):312e9.
- [44] Mauritz KA, Moore RB. State of understanding of Nafion. *Chem Rev* 2004;104(10):4535e85.

[45] Springer TE, Zawodzinski TA, Gottesfeld S. Polymer electrolyte fuel cell model. J Electrochem Soc 1991;138(8):2334e42.